# ADSORPTION OF NO ON LIGNIN-BASED ACTIVATED CARBONS WITH DIFFERENT POROUS STRUCTURE.

J.M. Rosas, D.J. Molina, A. Wucherpfening, J. Rodríguez-Mirasol, T. Cordero Chemical Engineering Department, School of Industrial Engineering, University of Málaga. Campus de El Ejido, s/n, 29013 Málaga, Spain.

Corresponding author e-mail address: mirasol@uma.es

#### Introduction

The emissions of nitrogen oxides  $(NO_x)$  from stationary and mobile sources are recognized to be precursors in the formation of acid precipitation and stratospheric ozone. Many studies have been made to develop highly effective technologies for NOx removal, as the direct reduction of NO and selective catalytic reduction (SCR). Attention has been recently focused on the developing of new catalyst which can degrade the gas to non-toxic ones.

Carbonaceous materials have been extensively studied by Mochida [1], Yang [2], and De Soete [3], where carbon acts as the reducing agent towards NO and  $N_2O$ . However, little information is available in the literature about the interaction between  $NO_x$  and the carbon surface. The presence of oxygen clearly enhances the rate of the reaction. Ashmed et.al [4] suggested that NO is oxidized by  $O_2$  to  $NO_2$  in the gas phase and then,  $NO_2$  is adsorbed onto the AC surface; however Rao and Hougen [5] found that the oxidation of NO in the gas phase is very low compared with that in the presence of AC. There are many contradictions about the influence of the porous structure of the carbon on this process as well. Shimizu et al. [6], Illán-Gómez [7] and Johnson [8] found a relationship between the reactivity of NO reduction by char and the internal surface area of the char. Nevertheless, Suzuki et al. [9] and Mochida et al. [10] found no relationship between surface area and activity in their studies.

The present work study the influence of the porous structure and the surface chemistry of different carbons on the NO adsorption

## **Experimental**

Several activation methods of lignin were carried out to obtain the substrates used in this study: Carbonization at 1073K;  $H_2O_v$ -partial gasification at 1073K for two hours; and chemical activation using  $ZnCl_2$  and  $H_3PO_4$  as activation agents, with impregnation ratios of 2.3, and 3, respectively, at 773 K during 2 hours. The different carbons were denoted by C800,  $ACH_2O$ ,  $ACZnCl_2$  and  $ACH_3PO_4$ , respectively.

The porous structure of the different substrates has been analyzed by adsorption-desorption of  $N_2$  at 77K, using a Coulter Omnisorp 100CX apparatus, and by  $CO_2$  adsorption at 273K in a Autosorb-1 system (Quantachrome). The surface chemistry of the carbons has been studied using temperature-programmed desorption (TPD)

analysis, with a Ultramat 22, Siemens model and by XPS analyzer 5700C model Physical Electronics apparatus with Mgk $\alpha$  radiation (1253.6 eV). The elemental analysis of the substrates were realized by a Leco CHNS-932 system

The adsorption experiments were performed in a fixed bed reactor at 293K and atmospheric pressure, using 100 mg of carbon sample for a total flow rate of 200 ml/min, with a concentration of 200 ppm of NO. NO and  $NO_2$  concentration was measured by a chemiluminiscent analyser (EcoPhysics, CLD 700 AL model), and the CO and  $CO_2$  concentrations by means of a non-dispersive infra-red analyzer (Ultramat 22, Siemens model).  $N_2O$  and  $N_2$  were analyzed with a mass spectrometer analyzer (Balzers MsCube).

#### **Results and discussions**

The structural parameters obtained from the  $N_2$  and  $CO_2$  adsorption isotherm are presented in Table 1. C800 presents a very narrow microporous structure, suggested by the low value of the apparent surface area measured with  $N_2$ ,  $A_{BET}$ , and a high value of the surface area deduced from the  $CO_2$  isotherm,  $A_{DR}$ .  $ACH_2O$  presents a microporous structure with high values of surface area derived from both  $N_2$  and  $CO_2$  adsorption data.  $ACZnCl_2$  presents a structure similar to that of  $ACH_2O$ , though with a wider porosity, suggested by a higher value of external surface area, At, and the differences observed between the micropore volume obtained from the  $N_2$  and  $CO_2$  data. Finally,  $ACH_3PO_4$  shows a porous structure with micropores and a large amount of mesopores.

Table 1. Surface properties of the different activated carbons.

	$A_{BET}$ (m <sup>2</sup> /g)	At (m <sup>2</sup> /g)	Vmes (cm <sup>3</sup> /g)	Vt (cm <sup>3</sup> /g)	$A_{DR}$ (m <sup>2</sup> /g)	$V_{DR}$ (m <sup>2</sup> /g)
C800	30	-	0.011	-	443	0.169
ACH <sub>2</sub> O	1174	60	0.045	0.482	989	0.377
ACZnCl <sub>2</sub>	1237	115	0.09	0.598	565	0.215
ACH <sub>3</sub> PO <sub>4</sub>	717	348	0.288	0.219	381	0.145

Table 2 shows the percentage of the different oxygen groups found on the surface of the carbons studied. Evolution of CO<sub>2</sub> was almost negligible during the TPD experiments for most of the carbons. ACH<sub>3</sub>PO<sub>4</sub> carbon presents the major amount of gas desorbed as carbonyl and quinone groups, mainly. ACZnCl<sub>2</sub> and ACH<sub>2</sub>O desorb similar amount of CO, mostly, from phenolyc and carbonyl groups, while quinones and carbonyls groups are the main responsible for the evolution of CO from C800 carbon.

Figure 1 shows the amount of NO adsorbed on different carbons as a function of time. The profile of these curves consist, clearly, of three steps: a first one where NO adsorption at 293 K takes place, in a flow of helium with 200 ppm of NO, until the saturation of the carbon, a second one in which the NO adsorption decreases due to the desorption in an helium flow at the adsorption temperature; and a third step with a further decrease of NO adsorption, corresponding to the TPD experiment.

Table 2. Surface oxigenated groups of the activated carbons.

Oxigenated	arouns	%
Oxigenated	groups	/0

Substrate	Anhydrides	Phenolycs	Carbonyls	Quinones	mg CO desorbed/g AC
C800	18.43	16.62	31.66	30.49	14.7
ACH2O	7.42	67.36	25.22	-	45.1
ACZnCl2	4.7	88.01	7.29	-	55.5
ACH3PO4	7.56	10.8	55.98	25.66	114.5

During the adsorption process, all the activated carbons present a lineal behavior at short times. The rate constant  $(k_o)$  obtained from this lineal section shows also a lineal relationship with the external surface area (At), which is in agreement with the results obtained by Illán-Gómez et.al [6] and Shimizu et.al [5]. It can also be observed from Figure 1, that the total amount of NO adsorbed is higher for substrates with high mesopores volume values  $(V_{mes})$ .

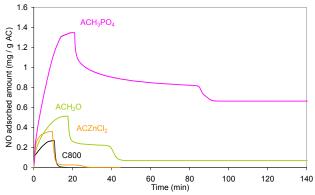


Figure 1. NO adsorbed amount as a function of time for different activated carbons during adsorption and desorption at 293K and TPD experiments. (NO concentration 200ppm; absence of oxygen in the inlet gas flow).

Figure 2 corresponds to an experimental sequence similar to the explained before for Figure 1, in which all the activated carbons, previously to the NO adsorption, were thermally treated up to 1173K in an inert gas atmosphere, in order to remove the oxygen complexes. The removing of the oxygen complexes enhances, significantly, the NO adsorbed amounts, in agreement with the observations of Yang et.al [2], Ahmed et.al [3].and Aarna and Suuberg [10], which suggests that the surface covered by oxygen complexes inhibits the adsorption (and probably the reaction) of NO on carbon at low temperatures.

Figure 3 shows that the presence of oxygen in the inlet gas flow improves the adsorption capacity of the carbons. It is also noteworthy to mention that not all the NO adsorbed is desorbed during the desorption at 273 K and the TPD experiments, which suggests that either reaction of NO is taking place to form other nitrogen species different to NO and NO<sub>2</sub> or nitrogen is been retained on the surface of the carbon.

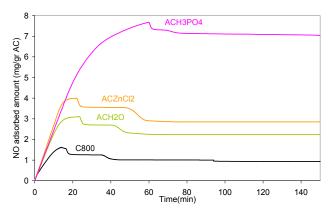


Figure 2. NO adsorbed amount as a function of time for different activated carbons during adsorption and desorption at 293K and TPD experiments. (NO concentration 200ppm; absence of oxygen in the inlet gas flow; the activated carbons were previously subjected to thermal treatment to remove the oxygen surface groups).

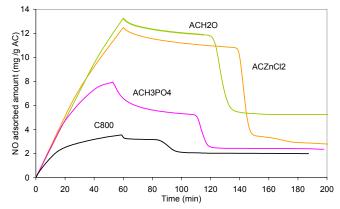


Figure 3. NO adsorbed amount as a function of time for different activated carbons during adsorption and desorption at 293K and TPD experiments. (NO concentration 200ppm; presence of oxygen (5%<sub>V</sub>) in the inlet gas flow; the activated carbons were previously subjected to thermal treatment to remove the oxygen surface groups).

The same experiments were carried out with 1500 ppm NO and 5%  $O_2$  in the inlet gas flow using the mass spectrometer (MS) system to analyze the possible formation of  $N_2$  and  $N_2O$ . Figure 4 shows the results obtained for adsorption-desorption at 293K and Figure 5 those for TPD experiment. The formation of  $NO_2$  during adsorption of NO in the presence of oxygen (Figure 4) starts, approximately, at about 60% of the NO adsorption capacity [14], indicating that oxidation of NO takes place during adsorption. Formation of small amount of  $N_2$  and  $CO_2$  at the very beginning of the adsorption process was also observed by MS (not shown), suggesting that the carbon surface may reduce NO at 293 K. No  $N_2O$  was observed during these experiments. Evolution of NO,  $NO_2$  and  $CO_2$  during the TPD experiments (Figure 5) at temperature higher than 293 K indicate that part of the NO oxidized during adsorption is chemisorbed on the carbon surface and part of the NO is strongly bonded to the carbon surface, needing higher temperatures to be desorbed from the surface.

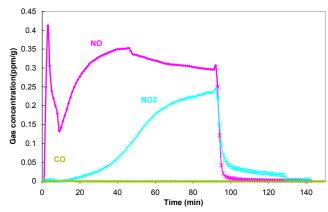


Figure 4. Gas concentration for adsorption at 293 K of NO (1500 ppm NO,  $5\%_V$  O<sub>2</sub>) on ACH<sub>2</sub>O carbon heat treated previously to high temperature to remove oxygen surface groups.

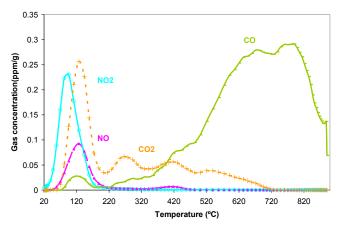


Figure 5. Gas concentration for the TPD experiment to ACH<sub>2</sub>O carbon after adsorption/desorption of NO at 293 K (1500 ppm NO, 5%<sub>V</sub> O<sub>2</sub>).

The amount of  $N_2$  detected by the MS system during the first step of adsorption is not enough to close the N balance. The results suggest that nitrogen is very strongly retained by the carbon, even after the heat treatment during the TPD experiments. Table 3 and 4 show the elemental and XPS analyses of the different carbons after adsorption of NO in the presence of  $O_2$  at 273 K (A), after adsorption (at the same conditions) and desorption at 293 K (A-D) and after adsorption-desorption at 293 K and further heat treatment during the TPD experiments. The amount of N found on the original carbons was negligible. The fact that N is still present on carbons where TPD has been carried out after adsorption of NO in the presence of oxygen confirms the hypothesis that N has been stabilized on the surface of the carbons during the adsorption process.

Table 3. Elemental analysis for different activated carbons: (A) after adsorption of NO at 293K; (A-D) after adsorption and desorption at 293K; (A-D-TPD) after adsorption, desorption and TPD. (Adsorption: 1500 ppm NO and 5%  $O_2$  in He. Desorption and TPD: He)

	С	Н	N	0
ACH2O A	73.9	3.1	2.6	20.4
ACH3PO4 A	70.4	1.8	1.5	26.3
ACH2O A-D	79.5	2	2.3	16.2
ACH3PO4 A-D	72.9	1.6	1.1	24.4
ACH2O A-D-TPD	98.2	0.6	0.7	0.5
ACH3PO4 A-D-TPD	80.4	1.4	0.5	17.7

Two different peaks for N1s can be observed for the carbons subjected to the different treatments above mentioned (Table 4). The peak corresponding to a binding energy value close to 406 eV can be assigned to N bonding to an electronegative element, i.e. a nitrate or nitrite group. The second peak, observed at a binding energy around 400.7 eV, has been ascribed to a C-N bond [17]. The increase of the percentage of the second peak after the TPD experiment indicates that N is mostly bonded to the carbon structure after the TPD experiments, although a significant amount of N bonded to oxygen is still present, most likely, in the narrowest micropores.

Table 4. XPS N1s binding energies and their relative percentage for different activated carbons: (A) after adsorption of NO at 293K; (A-D) after adsorption and desorption at 293K; (A-D-TPD) after adsorption, desorption and TPD. (Adsorption: 1500 ppm NO and 5% O<sub>2</sub> in He. Desorption and TPD: He).

	Binding Energy (eV)		Relative percentage (%)	
	Peak 1	Peak 2	Peak 1	Peak 2
ACH2O A	406.2	399.7	71.2	28.8
ACH3PO4 A	406.9	400.7	67.13	32.87
ACH2O A-D	406.2	399.7	70.71	29.29
ACH3PO4 A-D	406.1	400.9	64.06	35.94
ACH2O A-D-TPD	406.2	399.7	51.34	48.66
ACH3PO4 A-D-TPD	406.7	400.1	28.48	71.52

#### Conclusions

The removing of the oxygen complexes from the surface carbon increases significantly the amount of NO adsorbed. This enhancement is due to the oxygen surface groups desorbed as CO, specially to those desorbed a lower temperatures. The presence of oxygen improves the adsorption capacity of the carbons. Formation of  $CO_2$  and  $N_2$  seems to take place during the first step of adsorption at 293 K, probably, due to reduction of NO by the carbon surface. The results suggest that nitrogen is very strongly retained on the surface of the carbon, even after the heat treatment during the TPD experiments.

### References

- 1.- Mochida, I., Kawano, S., Hironaka, M., Yatsunami, S., Matsumura, Y., Energy and Fuels 9:659 (1995).
- 2.- Yang, J., Mestl, G., Herein, D., Schlögl, R., Find, J., Carbon 38: 715-727 (2000).
- 3.-Ahmed, S.N., Baldwin, R., Derbyshire, F., McEnaney, B., Stencel, J., Fuel 72: 287 (1993).
- 4.- Rao, M.N., Hougen, O.A., Chem Engng Prog Symp Ser 4:11 (1952).
- 5.- Shimizu, T., Sazawa, Y., Adschiri, T., Furusawa, T., Fuel 71:361-365 (1992).
- 6.- Illán-Gómez, M.J., Linares-Solano, A., Salinas-Martínez de Lecea, C., Colo, J.M., Energy and Fuels 7: 146-154 (1993).
- 7.- Johnson, J.E., Fuel 73:1398-1415 (1994).
- 8.- Suzuki, T., Kyotani, T., Tomita, A., Ind Engng Chem Res. 33: 2840-2845 (1994).
- 9.- Mochida, I., Ogaki, M., Fujitsu, H., Komastsubara, Y., Ida, S., Fuel 64: 1054-1057 (1985).
- 10.- Aarna, I., Suuberg, E.M., Fuel 76: 475-491 (1997).
- 11.- Zevenhoven, R., Huppa, M., Fuel 77: 1169-1176 (1998).
- 12.- Mochida, I., Kawano, S., Hironaka, M., Kishino, M., Yatsunami, S., Korai, Y., Yoshikawa, M., Chem Lett 385 (1995).
- 13.- Zhu, Z., Liu, Z., Liu, S., Niu, H., Fuel 79:651-658 (2000).
- 14.-Mochida, I., Shirahama, N., Kawano, S., Kora, Y., Yasutake, A., Tanoura, M., Fujii, S., Yoshikawa, M., Fuel 79: 1713-1723 (2000).
- 15.- Yang, J., Mestl, G., Herein, D., Schlögl, R., Find, J., Carbon 38: 729-740 (2000).
- 16.- Li, Y.H., Lu, G.Q., Rudolph, V., Chem Engng Science 53: 1-26 (1998).
- 17.- Rodríguez-Mirasol, J., Ooms, A.C., Pels, J.R., Kapteijn, F., Moulijn, J.A., Combustion and Flame 99: 499-507 (1994).
- 18.- Schmiers, H., Triebel, J., Strenbel, P., Hesse, R., Kopsel, R., Carbon 37: 1965-1978 (1999).
- 19.- Lahaye, J., Nanse, G., Bagreev, A., Strelko, V., Carbon 37: 585-590 (1999).
- 20.- Wu, Y., Fang, S., Jiang, Y., Solid Static Ionics 120: 117-123 (1999).